

INTRA-PARTICLE HEAT TRANSFER EFFECTS IN COAL PYROLYSIS

Mohammed R. Hajaligol, William A. Peters, and Jack B. Howard
Energy Laboratory and Department of Chemical Engineering,
M.I.T., Cambridge, MA 02139

May, 1987

Abstract

Time and spatial temperature gradients within pyrolyzing coal particles can exert strong effects on devolatilization behavior including apparent pyrolysis kinetics. This paper mathematically models transient spatial non-isothermality within an isolated, spherical coal particle pyrolyzing by a single first-order reaction. The analysis provides three distinct indices of heat transfer effects by quantitatively predicting the extent of agreement between: (a) centerline and surface temperature; (b) volume averaged pyrolysis rate [or (c) volume averaged pyrolysis weight loss] and the corresponding quantity calculated using the particle surface temperature for the entire particle volume. Regimes of particle size, surface heating rate, and reaction time where particle "isothermality" according to each of criteria (a) through (c) is met to within prescribed extents, are computed for conditions of interest in entrained gasification and pulverized coal combustion, including pyrolysis under non-thermally neutral conditions.

Introduction. Many coal combustion and gasification processes involve particle sizes and surface heating rates producing temporal and spatial temperature gradients within the coal particles during pyrolysis. These gradients may strongly influence volatiles yields, compositions, and release rates, and can confound attempts to model coal pyrolysis kinetics with purely chemical rate expressions. Mathematical modelling of particle non-isothermality is needed to predict reaction conditions (viz. particle dimension, surface heating rate, final temperature, and reaction time) for which intra-particle heat transfer limitations do not significantly influence pyrolysis kinetics, and to predict pyrolysis behavior when they do. When pyrolysis is not thermal-neutral, the analysis is non-trivial since local temperature fields are coupled non-linearly to corresponding local heat release (or absorption) rates and hence to local pyrolysis kinetics.

Much of the pertinent literature has addressed pseudo steady-state models for spatial temperature gradients within catalyst particles playing host to endo- or exothermic reactions, including, for some cases, mathematical treatment of the attendant limitations on intra-particle mass transfer of reactants or products [See Ref. (1) and references cited therein]. There appear to have been few analyses of non-isothermality within a condensed phase material simultaneously undergoing non-thermally neutral chemical reaction(s). Previous work includes rather empirical approaches to fitting coal weight loss kinetics [see reviews by Howard (2) and Gavalas (3)], and more refined analyses of spatial non-isothermality within exploding solids (4,5). Gavalas (2) calculated regimes of coal particle size where pyrolysis kinetics should be free of heat transfer effects, and Simmons (6) provided similar information for cellulose pyrolysis. Valuable contributions are also

emanating from the laboratories of Essenhigh (7), and Freihaut and Seery (8).

There is need for a generic, quantitative formalism to reliably predict transient intra-particle non-isothermality and their effects on pyrolysis, as a function of operating conditions of interest in modern fuels utilization technologies. To this end the present paper presents, for an isolated spherical coal particle pyrolyzing by a single first-order reaction, quantitative predictions of three distinct indices of particle non-isothermality - namely the extent of agreement between: (1) temperatures at the particle surface and centerline; (2) the pyrolysis rate [or (3) the pyrolysis weight loss] averaged over the particle volume and the corresponding quantity calculated using the particle surface temperature for the entire particle volume. Each index is explicitly dependent on time and thus accounts for the temporal as well as the spatial non-idealities in particle "isothermality".

Method of Analysis. Spatial limitations allow only a brief summary of the theoretical approach, which is described in more detail with broader applications, by Hajaligol et al. (9). For an isolated spherical coal particle with temperature invariant thermal physical properties, pyrolyzing by a single first-order endo or exo-thermic reaction with an Arrhenius temperature dependency, heated at its surface, and transmitting heat internally only by conduction, (or by processes well-described by an apparent isotropic thermal conductivity) a standard heat balance gives the following partial differential equation for the time and spatial dependence of the intra-particle temperature field

$$\frac{1}{\alpha} \left(\frac{\partial T}{\partial t} \right) = \frac{1}{r^2} \frac{\partial}{\partial r} \left(r^2 \frac{\partial T}{\partial r} \right) + \frac{(-\Delta H_{py}) f k_0 e^{-E/RT}}{\lambda} \quad (1)$$

Following Boddington et al. (1982) and others, this may be rewritten in dimensionless form as

$$\left(\frac{\partial \theta}{\partial \tau} \right) = \frac{1}{\xi^2} \frac{\partial}{\partial \xi} \left(\xi^2 \frac{\partial \theta}{\partial \xi} \right) + \delta \exp \left[\frac{\theta}{\beta + \epsilon \theta} \right] \quad (2)$$

Symbols are defined in the nomenclature section at the end of the paper. Solution of Equation (1) or (2) requires specification of one initial condition and two spatial boundary conditions. The initial condition prescribes the temperature field throughout the coal particle at the instant heating begins

$$T(r, 0) = T_0 \quad (3)$$

or

$$\theta(\xi, 0) = 1 \quad (4)$$

One boundary condition is the mathematical expression for centerline symmetry of the particle temperature field at all pyrolysis times

$$\left(\frac{\partial T}{\partial r} \right)_{r=0} = 0 \quad (5)$$

or

$$\left(\frac{\partial \theta}{\partial \xi} \right)_{\xi=0} = 0 \quad (6)$$

Four cases are of interest for the second boundary condition in the present analysis:

(1) A finite rate of heat transmission to the particle surface describable in terms of an apparent heat transfer coefficient

$$-\lambda \left(\frac{\partial T}{\partial r} \right)_{r=R_0} = h_{\text{eff}} (T - T_{\infty}) \quad (7)$$

or

$$\left(\frac{\partial \theta}{\partial \xi} \right)_{\xi=1} = -N_{\text{Bi}} (\theta - \theta_{\infty}) \quad (8)$$

This case would be applicable to heating of coal particles in a fluidized bed or by molecular conduction from a high temperature gas. It also automatically accommodates cases where the overall rate of heat transfer to the particle is influenced by extra-particle resistance [i.e. cases of non-infinite Biot number].

(2) A prescribed constant rate of increase in the particle surface temperature:

$$T_s(t) = T_0 + \dot{m} t \quad (9)$$

or

$$\theta_s(\tau) = 1 - \gamma \tau \quad (10)$$

This case is applicable to screen heater reactors or other apparatus where surface heating rates are maintained essentially constant.

(3) A known, constant surface heat flux density:

$$-\lambda \left(\frac{\partial T}{\partial r} \right)_{r=R_0} = \dot{q} / 4\pi R_0^2 \quad (11)$$

or

$$\left(\frac{\partial \theta}{\partial \xi} \right)_{\xi=1} = -\Phi \quad (12)$$

This case is especially applicable to fires and furnaces under conditions where the particle surface temperature remains well below the temperature of the surroundings, and sample heating is dominated by radiation.

(4) A special limiting case of (1) through (3) above is an infinitely rapid surface heating rate:

$$T_s^1(t) = T_s^1(\infty) , \quad r = R_0 \quad (13)$$

or

$$\Theta_s(\tau) = 0 , \quad \xi = 1 \quad (14)$$

This case would approximate the heat transfer characteristics of systems providing very rapid surface heating of the coal particles, for example shock tubes, laser and flash lamp reactors, and coal dust explosions, where surface heating rates are estimated to exceed $10^5 - 10^7$ C/s.

Equations (1) and (2) were solved numerically for each of the above four cases of boundary condition, using a procedure based on the method of lines and on Gear's method. Only our results for constant surface heating rate, Case (2) above, will be presented here. Results for other cases are presented by Hajjaligol et al. (9).

The solutions to these two equations are predictions of the spatial variation of the intra-particle temperature field with pyrolysis time. This information was used to compute three distinct indices of particle non-isothermality:

(1) The extent of agreement between the surface and centerline temperature of the particle:

$$\eta_T(t) = [T_s^1(t) - T_{cL}^1(t)] / T_s^1(t) \quad (15)$$

or

$$\hat{\eta}_T(\tau) = \Theta_{cL}(\tau) - \Theta_s(\tau) \quad (16)$$

(2) A time dependent effectiveness factor for pyrolysis rate, defined as the ratio of: the local pyrolysis rate averaged over the particle volume, to the pyrolysis rate calculated using the particle surface temperature for the entire particle volume:

$$\eta_r(t) = \frac{\frac{1}{V} \int_V k_0 e^{-E/RT(v,t)} dv}{k_0 e^{-E/RT_s^1(t)}} \quad (17)$$

or

$$\hat{\eta}_r(\tau) = \frac{3 \int_0^1 k_0 e^{-\frac{\beta}{\beta E + E^2 \Theta(\xi, \tau)}} \xi^2 d\xi}{k_0 e^{-\beta/(\beta E + E^2 \Theta_s(\tau))}} \quad (18)$$

(3) A time-dependent effectiveness factor for overall pyrolytic conversion (i.e. weight loss or total volatiles yield) defined as the ratio of: the volume averaged weight loss, to the weight loss calculated using the particle surface temperature for the entire particle volume:

$$\zeta_c(t') = \frac{1 - \frac{1}{V} \int_V \left\{ \exp \left[- \int_0^{t'} k_0 e^{-E/RT(v,t)} dt \right] \right\} dV}{1 - \left\{ \exp \left[- \int_0^{t'} k_0 e^{-E/RT_s(t)} dt \right] \right\}} \quad (19)$$

or

$$\hat{\zeta}_c(\tau') = \frac{1 - 3 \int_0^{\tau'} \left\{ \exp \left[- \int_0^{\tau'} \phi e^{-\beta/[\epsilon\beta + \epsilon^2\theta(\delta,\tau)]} d\tau \right] \right\} d\delta}{1 - \left\{ \exp \left[- \int_0^{\tau'} \phi e^{-\beta/[\epsilon\beta + \epsilon^2\theta_s(\tau)]} d\tau \right] \right\}} \quad (20)$$

Results and Discussion. The above analysis was used with boundary condition (2) [constant surface heating rate] to predict effects of various pyrolysis parameters on $\eta_T(t)$, $\eta_R(t)$, and $\eta_C(t)$ as a function of pyrolysis time. Unless otherwise stated the following values of thermal physical and chemical properties of the coal were employed: $\rho = 1.3 \text{ g/cm}^3$, $\lambda = 0.0006 \text{ cal/cm-s-C}$, $C_p = 0.4 \text{ cal/g-C}$, $\Delta H_p = 0 \text{ cal/g}$, $k_0 = 10^{13} \text{ s}^{-1}$, and $E = 50 \text{ kcal/g-mole}$. Effects of non-zero heats of pyrolysis are discussed later in the paper.

Figures 1 - 3 respectively show the effects of particle size on $\eta_T(t)$, $\eta_R(t)$, and $\eta_C(t)$, for a surface heating rate and final temperature of 10^4 C/s and 1000 C . For particle sizes $> 50 \mu\text{m}$, the time to relax internal temperature gradients [i.e. for $\eta_T(t)$ to decline from its maximum value to about zero] increases with roughly the square of particle diameter as expected. Initially the spatial non-idealities in temperature (Fig. 1) increased with increasing pyrolysis time, because the time for the surface to reach the final temperature [$T_{s,f}/m$] is much less than the particle thermal response time, and the intra-particle temperature field is unable to keep pace with the rapidly rising surface temperature. The magnitude and duration of this initial temperature transient increases with particle diameter, because the particle thermal response time increases with particle size.

The rate index of non-isothermality, $\eta_T(t)$ (Figure 2) tracks the non-idealities in particle temperature. For a given particle size and thermally neutral reactions $\eta_R(t)$ indicates spatially non-isothermal kinetic behavior [i.e. $\eta_R(t) < 1$] over a broader range of pyrolysis times than does $\eta_T(t)$ [i.e. for which $\eta_T(t) > 0$, Fig. 1]. The rate index expresses the influence of the temperature non-idealities on the predicted volume averaged pyrolysis rates via an exponential function. Thus an amplification of the magnitude and duration of the temperature non-idealities is not surprising. Furthermore, when volatiles release rates are of interest, $\eta_T(t)$ is clearly a more reliable index of particle non-isothermality than is $\eta_T(t)$.

The conversion index of non-isothermality, $\eta_C(t)$ (Fig. 3), reflects the non-idealities in rate, and the exponential increase in conversion with total pyrolysis time. The latter effect attenuates the former at short and long pyrolysis times by respectively, denying and supplying the reaction adequate time to attain completion at the imposed heating rate. Thus for each particle size there is an intermediate range of reactions times throughout which the strong non-idealities in pyrolysis rate (Fig. 2) contribute major non-idealit-

ies in conversion (Fig. 3). The exponential dependencies of conversion on rate and reaction time, also cause the magnitude of $\eta_r(t)$ to change rapidly with pyrolysis time, resulting in the sharp variations in this index depicted in Fig. 3. Clearly, in light of the differences in Figures 1 through 3, when total volatiles yield is of interest, $\eta_r(t)$ is the preferred index of non-isothermality over either $\eta_T(t)$ or $\eta_c(t)$.

Figure 4 shows that at a fixed particle size, increasing the surface heating rate increases the magnitude but decreases the duration of the initial non-idealities in the particle temperature field. The first effect arises because, with increasing surface heating rate, the surface temperature increases so rapidly during a time equal to the thermal response time of the particle, that the intra-particle temperature field lags further and further behind the surface temperature. The shorter relaxation time arises because the higher initial temperature gradients generated at higher surface heating rates cause a more rapid attenuation of the initial disturbance. With increasing heating rate, these sharp initial intra-particle temperature gradients translate into strong non-idealities in the local pyrolysis rates and hence into significant departures of $\eta_r(t)$ from unity (Fig. 5). With declining heating rates (Fig. 5) the magnitude of these non-idealities is attenuated but they remain significant over increasing ranges of pyrolysis time. These effects respectively arise because decreasing the surface heating rate reduces the differences between the surface and internal temperatures (Fig. 4), and because the resulting intra-particle temperature gradients are lower, and thus provide less driving force for temperature relaxation, thereby extending the time over which the intra-sample pyrolysis rates exhibit significant non-idealities. Increasing particle size at a fixed heating rate exacerbates each of the above effects (Fig. 2).

The impacts of these intra-sample rate variations on the conversion index of non-isothermality $\eta_r(t)$, are attenuated strongly in both magnitude and duration (Fig. 6), due to the interplay of rate and cumulative pyrolysis time discussed above. The magnitude of the non-idealities in $\eta_r(t)$ are worsened with increasing heating rate, because surface temperature and surface pyrolysis rate more and more rapidly outpace the corresponding quantities within the particle, thus expanding the differences between the extents of conversion predicted for these two regions at smaller and smaller reaction times. Conversely, the non-idealities in $\eta_r(t)$ decrease when heating rate decreases, because the particle temperature field (Fig. 4), and average pyrolysis rate (Fig. 5), track the surface temperature more and more closely, and because the greater time required for the surface temperature to attain its final value, allows intra-particle conversion to proceed further to completion.

For a thermally neutral reaction, a change in the activation energy for pyrolysis has no effect on intra-particle temperature gradients (and hence on $\eta_T(t)$), but Figure 7 shows that increasing E increases the magnitude of the non-idealities in $\eta_r(t)$, as would be expected since larger E 's imply stronger dependencies of rate on temperature. Since $\eta_r(t)$ is unaffected by changing E , any effect of E on $\eta_r(t)$ will reflect only E -induced changes in $\eta_c(t)$. Such effects should be small since at this heating rate (10^3 C/s) quite large changes in $\eta_r(t)$ at an E of 50 kcal/g-mole (Fig. 5), are strongly attenuated in $\eta_r(t)$ (Fig. 6), and the E -induced variations in $\eta_r(t)$ (Fig. 7) are by comparison, rather small.

Figure 8 shows that for constant ρ and C_p , decreasing either the thermal conductivity or thermal diffusivity of the coal increases the magnitude and duration of non-idealities in $\eta_T(t)$ and $\eta_C(t)$. For an endothermic reaction the values of $\eta_T(t)$ and $\eta_C(t)$ at long pyrolysis times would increase with increasing values of either of these thermal parameters. For example, for $\Delta H_p = +50$ cal/g coal, these two indices would increase by a factor of 10, for 10 to 15% increases in α or λ (Hajaligol et al. 1987).

Figure 9 shows the effects of pyrolysis time on $\eta_T(t)$, $\eta_C(t)$, and $n(t)$ for cases where pyrolysis is not thermal neutral. The discussion is simplified by expressing the results in terms of a dimensionless parameter δ , which reflects the interaction of chemical kinetic and thermal physical parameters in determining the impact of chemical enthalpy on particle non-isothermality. Delta is derived by non-dimensionalizing Eq. (1), see Eq. (2), and physically can be thought of as the ratio of the average rate of heat generation (or depletion) at the particle surface from pyrolysis, to the average rate of conductive transfer of heat into the particle from its surface. Figure 9 shows that for reasonable exo- or endo-thermicities, $\eta_T(t)$ and $\eta_C(t)$ do not approach perfect ideality, even at long pyrolysis times, while $\eta_C(t)$ goes virtually to unity (isothermal behavior) in reasonable times. The magnitude and duration of the non-idealities expressed by $\eta_C(t)$ depend on the ratio of the pyrolysis time to the particle heat-up time (Hajaligol et al. 1987). At long pyrolysis times $\eta_T(t)$ and $\eta_C(t)$ attain δ -specific plateaus that are independent of heating rate or particle size, although both parameters affect the magnitude and duration of the transients in these two indices.

Figure 10 shows, for thermally neutral pyrolysis, domains of particle size and surface heating rate where the particle is at least 95% "isothermal" according to each of the above indices [$\eta_T(t)$, $\eta_C(t)$, and $\eta_C(t)$]. The temperature index provides a broader range of compliant particle sizes and heating rates, because it is uninfluenced by devolatilization kinetics. For a non-thermally-neutral reaction it is much more difficult to define domains of particle size and heating rate where $\eta_T(t)$ meets the 95% ideality criterion - note the very small δ values required for $\eta_T(t)$ to approach 0 in Fig. 9.

The rate index [$\eta_T(t)$] obviously enfolds kinetic effects, and consequently presents a more narrow domain of isothermality (Fig. 10). Clearly this index, rather than $\eta_C(t)$ alone, should be considered in evaluating the role of heat transfer effects in devolatilization kinetic data and in designing experiments to probe intrinsic chemical rates. The conversion index, $\eta_C(t)$, provides a somewhat broader isothermality domain, due to the damping effect of pyrolysis time discussed above.

Effects of activation energy and thermal physical properties on the isothermality domains can be inferred from Fig.'s 7 and 8 respectively. Increasing or decreasing E as in Fig. 7, has no effect on the regions prescribed by $\eta_T(t)$ and $\eta_C(t)$, but respectively decreases and increases the domains defined by $\eta_T(t)$ (dashed lines of Fig. 10).

When pyrolysis is not thermally neutral, the domains of particle isothermality may, depending on the magnitude of ΔH_p , shrink from the boundaries defined in Fig. 10. Regimes of D_p and \dot{m} meeting each of the above criteria can still be prescribed by calculating compliant families of curves in Fig. 10, using ΔH_p as a parameter. Alternatively, the parameter δ can be used to

advantage in a more efficient computation procedure that accounts explicitly for all parameters contributing to heat of pyrolysis effects. The rate index, $\eta_r(t)$ shows the greatest effect of ΔH_p , (Fig. 9). Figure 11 shows how $\eta_r(t)$ varies with $|\delta|$, where the upper and lower branches [$\eta_r(t) > 1$, and < 1], reflect exo- and endo-thermic pyrolysis, respectively. This figure is used to obtain values of δ such that $\eta_r(t)$ indicates a desired extent of isothermality, say 95%. With δ fixed, and fixed thermal-physical properties, the particle diameter, D_p , final surface temperature T_s , and surface heating rate, m , become the only adjustable parameters of the system. For preselected particle diameters, Fig. 10 is then used to define the allowed maximum surface heating rates for any of the isothermality indices, and the value from Fig. 11 sets the corresponding maximum allowed surface temperature. Alternatively a desired surface heating rate can be pre-selected with the corresponding maximum allowed particle diameter and surface temperature being obtained from Figs. 10 and 11 (via δ) respectively, or a maximum surface temperature can be pre-chosen with the compliant δ value (Fig 11) prescribing the maximum allowed D_p , and Fig. 10 the corresponding maximum acceptable surface heating rate. This protocol is conservative in that it is valid for all pyrolysis times, and utilizes the most stringent of the above isothermality indices, $\eta_r(t)$.

Conclusions

1. The extent of coal particle non-isothermality at any stage of pyrolysis can be quantitatively depicted in terms of numerical indices reflecting not only spatial non-uniformities of the intra-particle temperature field, but also non-idealities in the rate and extent of pyrolysis.
2. Mathematical modeling of coupled rates of intra-particle pyrolysis and heat transmission, relates each index to operating conditions of interest in coal combustion and gasification including surface heating rate, particle diameter, final temperature, and pyrolysis time.
3. Domains of surface heating rate and particle diameter where each isothermality criterion is met to within 5% at all pyrolysis times are plotted for a base case of zero heat of pyrolysis.
4. Data and procedures for using these same isothermality maps when pyrolysis is not thermal neutral are also provided.
5. The analysis shows that diagnosing a pyrolyzing coal particle as "isothermal" based upon close agreement between its surface and centerline temperature, can lead to serious errors in estimates of corresponding volatiles release rates and total volatiles yields.
6. Each isothermality index exhibits significant temporal variations, showing that pyrolysis time, and hence extent of conversion must be considered in assessing particle non-isothermality and its impact on pyrolysis behavior.

Nomenclature

d_p	Particle Diameter, Cm
E	Activation Energy, Cal/g-mole
h_{eff}	Effective Heat Transfer Coefficient, Cal/(Cm ² -Sec-C)
k	Reaction Frequency Factor, sec ⁻¹
\dot{m}	Surface Heating Rate, °K/sec
N_{Bi}	Biot Number; $h_{eff} d_p / 2\lambda$
\dot{q}	Surface Heat Flux Density, Cal/sec
R	Gas Constant; 1.987 Cal/gmole°K
r	Radius, Cm
R_o	Partice Radius, Cm
T	Temperature, °K
T_o	Initial Temperature, °K
T_s	Surface Temperature, °K
$T_{s,f}$	Final Surface Temperature, °K
T_∞	Ambient Temperature, °K
t	Time, Sec
V	Particle Volume, Cm ³
ρ	Particle Density, g/cm ³
λ	Particle Thermal Conductivity, Cal/(Cm-Sec-C)
α	Particle Thermal Diffusivity, Cm ² /Sec
ΔH_{py}	Heat of Pyrolysis, Cal/g
θ	Dimensionless Temperature; $\frac{T - T_{s,f}}{T_o - T_{s,f}}$
θ_s	Dimensionless Surface Temperature; $\frac{T_s(t) - T_{s,f}}{T_o - T_{s,f}}$
θ_{CL}	Dimensionless Center Temperature; $\frac{T_{CL}(t) - T_{s,f}}{T_o - T_{s,f}}$
θ_∞	Dimensionless Ambient Temperature; $\frac{T_\infty - T_{s,f}}{T_o - T_{s,f}}$
τ	Dimensionless Time; $\alpha t / R_o^2$
ξ	Dimensionless Length; r / R_o

$\eta_T, \hat{\eta}_T$	Dimensionless Temperature Index
$\eta_r, \hat{\eta}_r$	Dimensionless Rate Index
$\eta_c, \hat{\eta}_c$	Dimensionless Conversion Index
ϵ	Dimensionless Parameter; $R T_{s,f} / E$
β	Dimensionless Parameter; $R T_{s,f}^2 / E (T_0 - T_{s,f})$
δ	Dimensionless Parameter; $(-\Delta H_{py}) \rho d_p^2 k_c e^{-\epsilon/R T_{s,f}} / [4 \lambda (T_0 - T_{s,f})]$
γ	Dimensionless Heating Rate; $\dot{m} d_p^2 / [4 \alpha (T_0 - T_{s,f})]$
Φ	Dimensionless Heat Flux Density; $\dot{q} / [2 \pi \lambda d_p (T_0 - T_{s,f})]$

Acknowledgements

Prime U.S.D.O.E. support for this work was provided via Contract No. DE-AC22-84PC70768, from the AR & TD Combustion Program of the Pittsburgh Energy Technology Center. Additional U.S.D.O.E. support was provided under Contract No. DE-AC21-85MC222049, from the Advanced Gasification Program of the Morgantown Energy Technology Center.

References

1. Froment, G. F., and K. B. Bischoff, Chemical Reactor Analysis & Design, John Wiley and Sons, 1979.
2. Howard, J. B., Fundamentals of Coal Pyrolysis and Hydrolyrolysis, in Chemistry of Coal Utilization, 2nd Suppl. Vol., Wiley NY 1981.
3. Gavalas, G. R., Coal Pyrolysis, Elsevier Scientific Pub., 1982.
4. Boddington, T., P. Gray, and S. K. Scott, J. Chem. Soc., Faraday Trans. 2, 78, 1721-1730, 1982.
5. Scott, S. K., T. Boddington, and P. Gray, Chem. Eng. Science, Vol. 39, No. 6, 1079-1085, 1984.
6. Simmons, G.M., Am. Chem. Soc., Div. of Fuel Chem. Preprints, April 1984.
7. Essenhigh, R.H., Dept. of Mechanical Eng., Ohio State University, Work in Progress, 1987.
8. Seery, D. J., J. D. Freihaut, and W. M. Proscia, Technical Progress Reports for DOE, 1985-1986, United Technologies Research Center, E. Hartford, CT.
9. Hajaligol, M. R., J. B. Howard, and W. A. Peters, Predicting Temporal and Spatial Non-Isothermalities within Reacting Condensed Phase Media, To be Submitted to the AIChE journal, 1987.

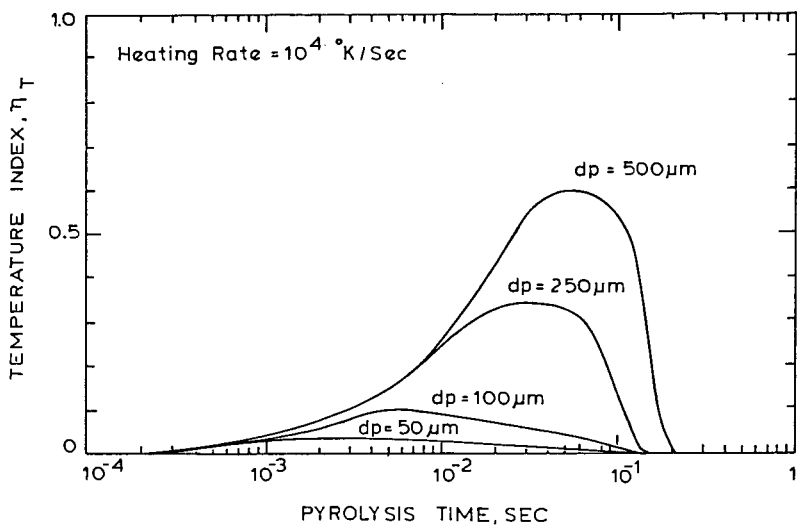


Figure 1. Effects of Particle Diameter on the Temperature Index at 10^4 K/sec Heating Rate.

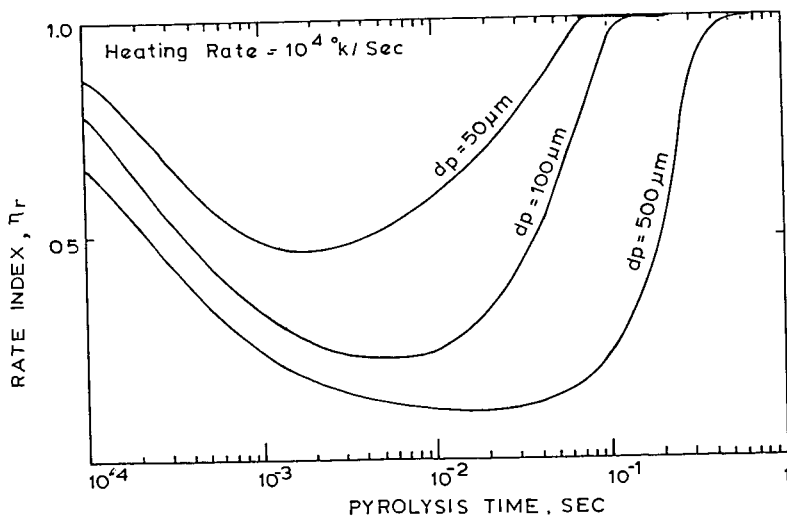


Figure 2. Effects of Particle Diameter on the Rate Index at 10^4 K/sec Heating Rate.

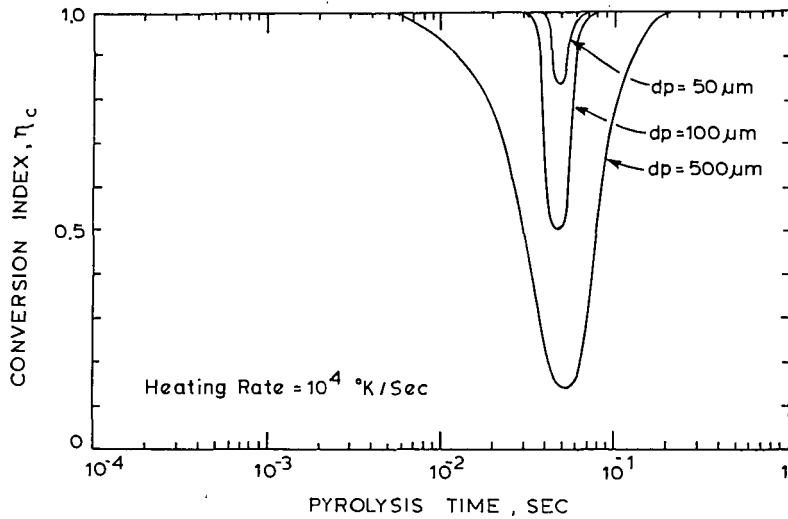


Figure 3. Effects of Particle Diameter on the Conversion Index at 10^4 K/sec Heating Rate.

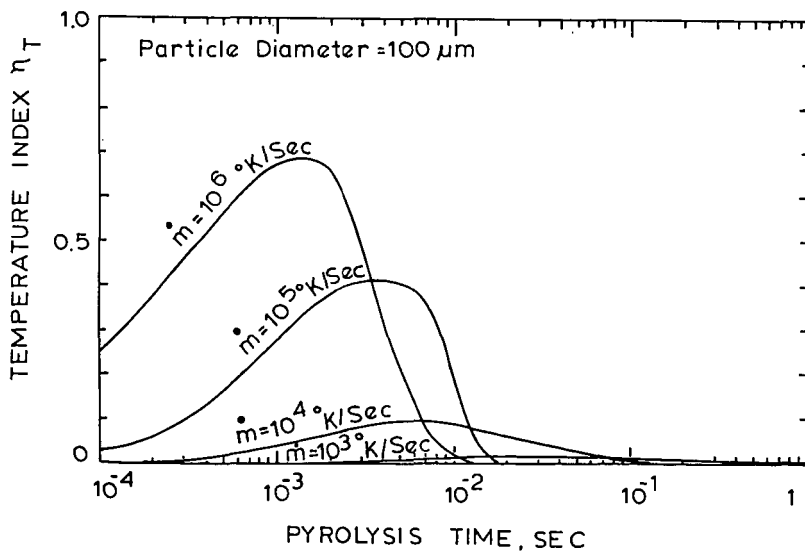


Figure 4. Effects of Heating Rate on the Temperature Index for 100 μm Particle Diameter.

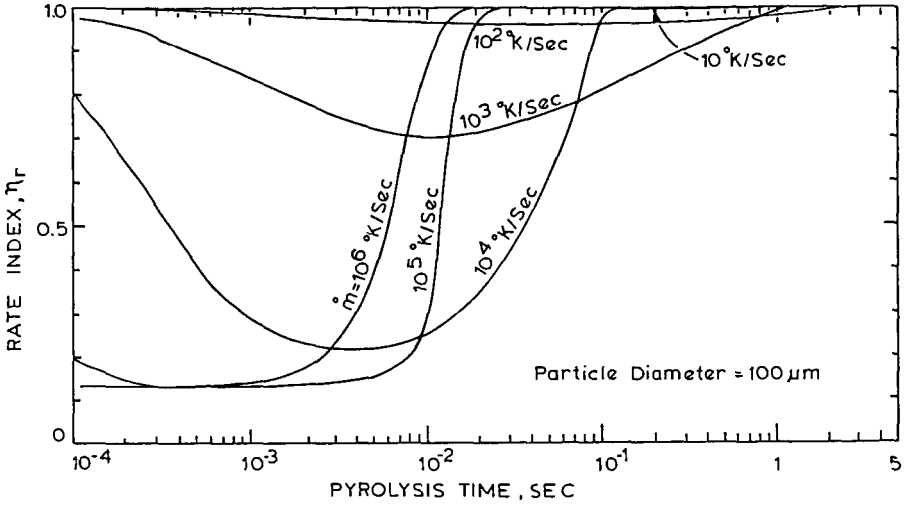


Figure 5. Effects of Heating Rate on the Rate Index for 100 μm Particle Diameter.

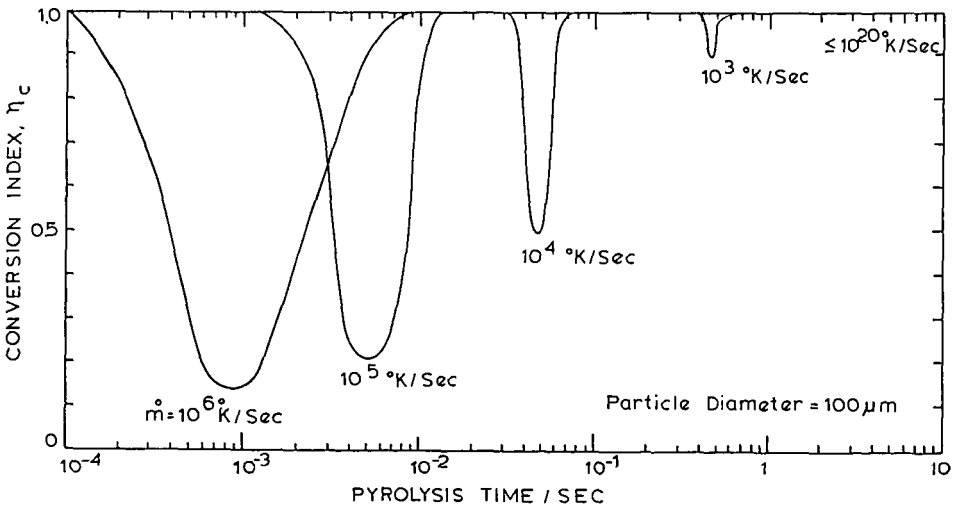


Figure 6. Effects of Heating Rate on the Conversion Index for 100 μm Particle Diameter.

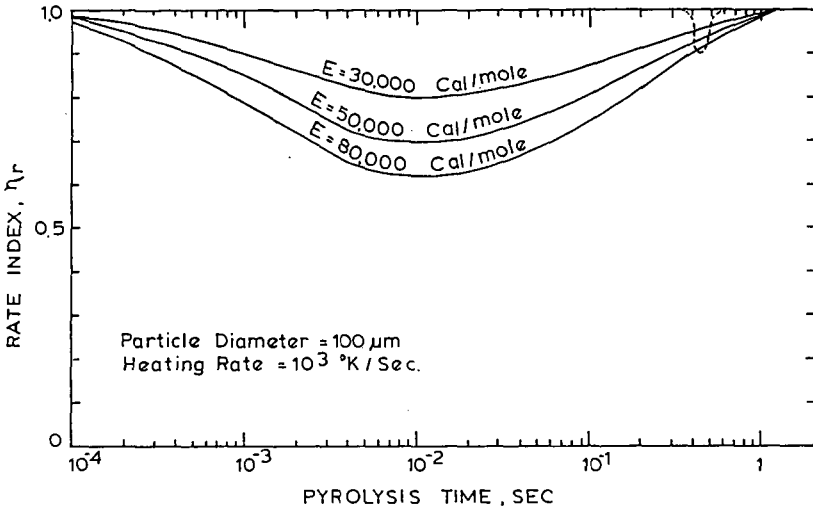


Figure 7. Effects of Activation Energy on the Rate and Conversion Indices.

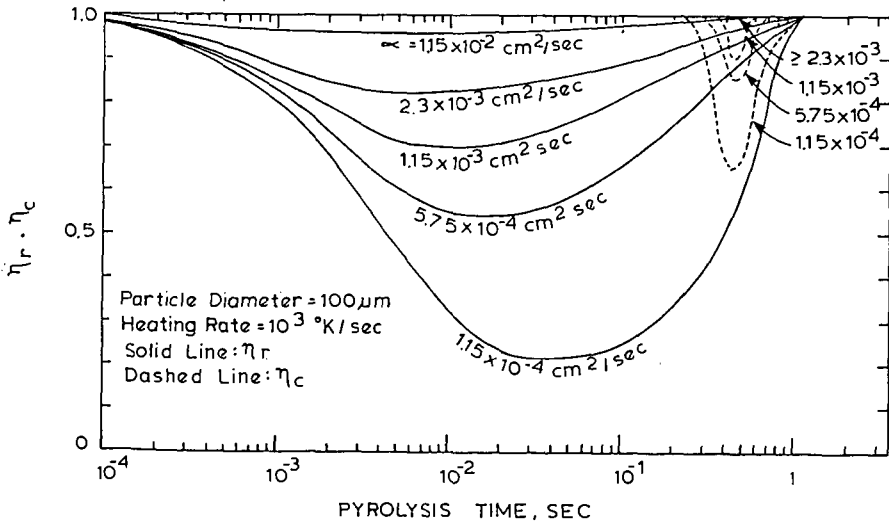


Figure 8. Effects of Thermal Diffusivity on Rate and Conversion Indices.

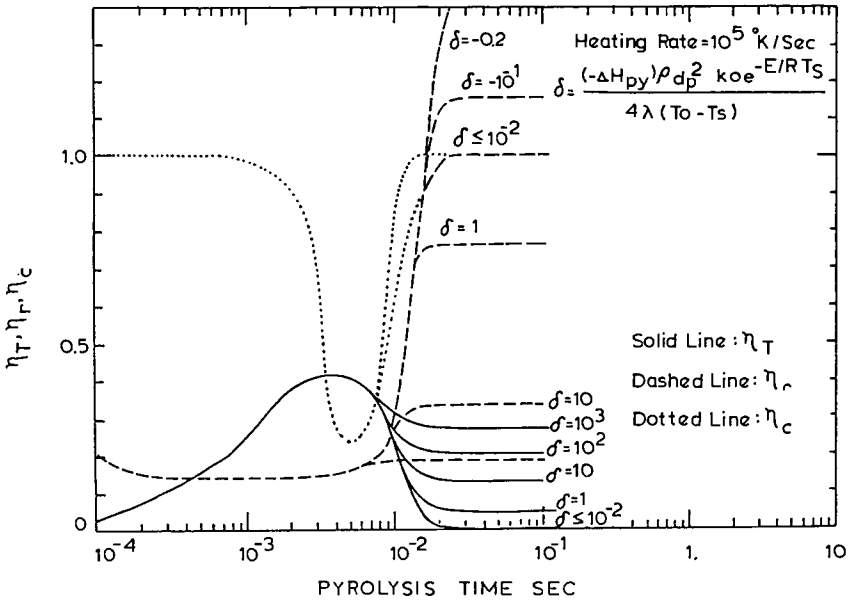


Figure 9. Effects of Heat of Pyrolysis on Indices.

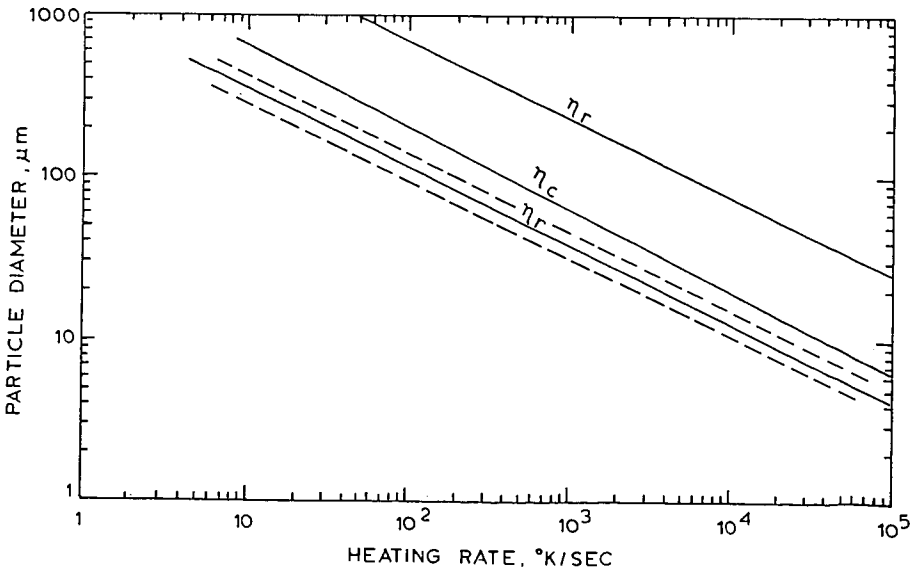


Figure 10. Isothermal Regions Defined by Different Indices.

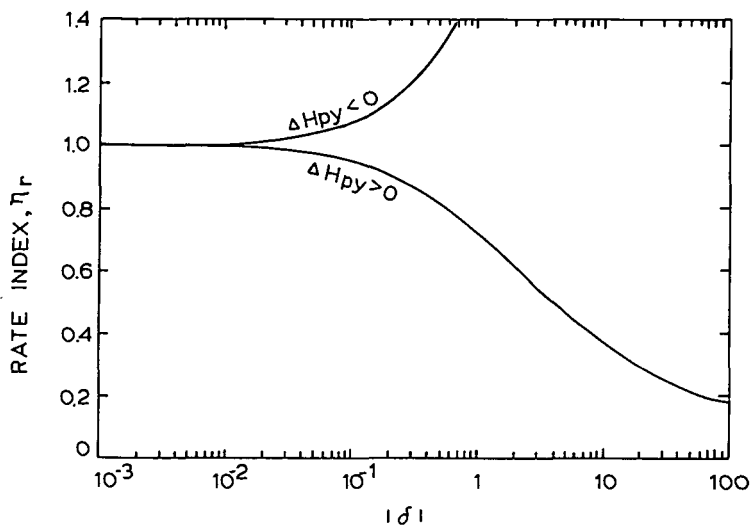


Figure 11. Effects of Heat of Pyrolysis on the Spatial Value of Rate Index.